Immobilized Furanone Derivatives as Inhibitors for Adhesion of Bacteria on Modified Poly(styrene-co-maleic anhydride)

ARTICLE *in* BIOMACROMOLECULES · SEPTEMBER 2012

Impact Factor: 5.75 · DOI: 10.1021/bm300932u · Source: PubMed

5 AUTHORS, INCLUDING:

Nonjabulo Prudence Gule
Stellenbosch University
12 PUBLICATIONS **37** CITATIONS
SEE PROFILE

Osama Bshena
Stellenbosch University
3 PUBLICATIONS **34** CITATIONS
SEE PROFILE

Thomas Eugene Cloete
Stellenbosch University
156 PUBLICATIONS **2,811** CITATIONS
SEE PROFILE

Bert Klumperman
Stellenbosch University
191 PUBLICATIONS **4,658** CITATIONS
SEE PROFILE

Article

pubs.acs.org/Biomac

Immobilized Furanone Derivatives as Inhibitors for Adhesion of Bacteria on Modified Poly(styrene-*co*-maleic anhydride)

Nonjabulo P. Gule,[†] Osama Bshena,[†] Michèle de Kwaadsteniet,[‡] Thomas E. Cloete,[‡] and Bert Klumperman[†,*]

[†]Division of Polymer Science, University of Stellenbosch, Stellenbosch, South Africa

[‡]Department of Microbiology, University of Stellenbosch, Stellenbosch, South Africa

ABSTRACT: The ability of brominated furanones and other furanone compounds with 2(3H) and 2(5H) cores to inhibit bacterial adhesion of surfaces as well deactivate (destroy) them has been previously reported. The furanone derivatives 4-(2-(2-aminoethoxy)-2,5-dimethyl-3(2H)-furanone and 5-(2-(2-aminoethoxy)-ethoxy)methyl)-2(5H)-furanone were synthesized in our laboratory. These furanone derivatives were then covalently immobilized onto poly(styrene-*co*-maleic anhydride) (SMA) and electrospun to fabricate nonwoven nanofibrous mats with antimicrobial and cell-adhesion inhibition properties. The electrospun nanofibrous mats were tested for their ability to inhibit cell attachment by strains of bacteria commonly found in water (*Klebsiella pneumoniae* Xen 39, *Staphylococcus aureus* Xen 36, *Escherichia coli* Xen 14, *Pseudomonas aeruginosa* Xen 5, and *Salmonella tymphimurium* Xen 26). Proton nuclear magnetic resonance spectroscopy (^{1}H NMR), electrospray mass spectroscopy (ES-MS), and attenuated total reflectance Fourier transform infrared spectroscopy (ATR-FTIR) were used to confirm the structures of the synthesized furanones as well as their successful immobilization on SMA. To ascertain that the immobilized furanone compounds do not leach into filtered water, samples of water, filtered through the nanofibrous mats were analyzed using gas chromatography coupled with mass spectroscopy (GC-MS). The morphology of the electrospun nanofibers was characterized using scanning electron microscopy (SEM).

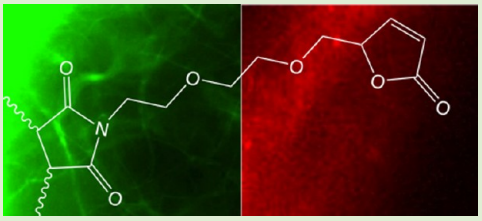

INTRODUCTION

The use of membrane technology in filtration systems is a promising technology. However, its large-scale industrial applicability is limited largely because of fouling of the membranes. Of all the types of fouling, biofouling which is caused by the attachment of microorganisms on membrane surfaces, is hardest to control. Chemical biocides such as chlorine have been used for decades to control biofouling of membranes.[1−5] Most of these chemical biocides are, however, not very effective at higher pH values and can react to form harmful byproducts.[6] Physical means to clean membranes have been reported, but only work best as secondary methods to other biofilm removal methods.[7] Other methods such as the use of bacteriophages, electrical current, and nutrient control have been explored, but these can take a long time to be effective and are in most instances very host specific.[8−10]

The focus is now moving to modification of membrane surfaces in order to control fouling. The modification of polymers by incorporating metal elements has been reported.[11,12] The application of these nanofibrous mats for wound dressing and filter media has been evaluated.[13] Muñoz-Bonilla and Fernández-Garćia reported on a wide range of polymeric materials with antimicrobial activity.[14] In their review, they highlighted five classes of polymers that have been found to have antimicrobial properties: polymers with quaternary nitrogen atoms, guanidine containing polymers, polymers that mimic natural peptides, halogenated polymers, and polymers containing phospho and sulpho derivatives.[14]

A class of compounds, collectively known as furanones, has been reported in the literature to possess the ability to inhibit surface colonization by microorganisms as well as antimicrobial properties against a wide range of microorganisms.[15−22] A good example of this phenomenon is observed in the marine algae *Delisea pulchra*, which does not get colonized by marine organisms. Furanones do this through suppression of a process called quorum sensing (QS). QS is a process by which bacteria communicate, and forms an essential part of biofilm formation. QS is not necessary for bacterial survival but helps in coordinating the community-based bacterial behavior, and even though interference with QS may not bring about a universally beneficial effect, it makes the bacteria more susceptible to control/destruction by traditional means. Biochemical studies to understand different pathways of QS have been carried out.[23,24] Furanone derivatives have been isolated from nature and have also been synthesized. Specific QS routes for these furanone derivatives have been reported.[25−27] Research on clinical applications of furanone compounds is widespread.[22,28−30]

In a recent article, inhibition of QS by the furanone moiety was reported to have prevented soft rot caused by *Pseudomonas aeruginosa* from attacking onion plants.[31] This shows the potential and wide applicability of furanone-mediated QS

Received: June 19, 2012
Revised: August 29, 2012
Published: September 4, 2012

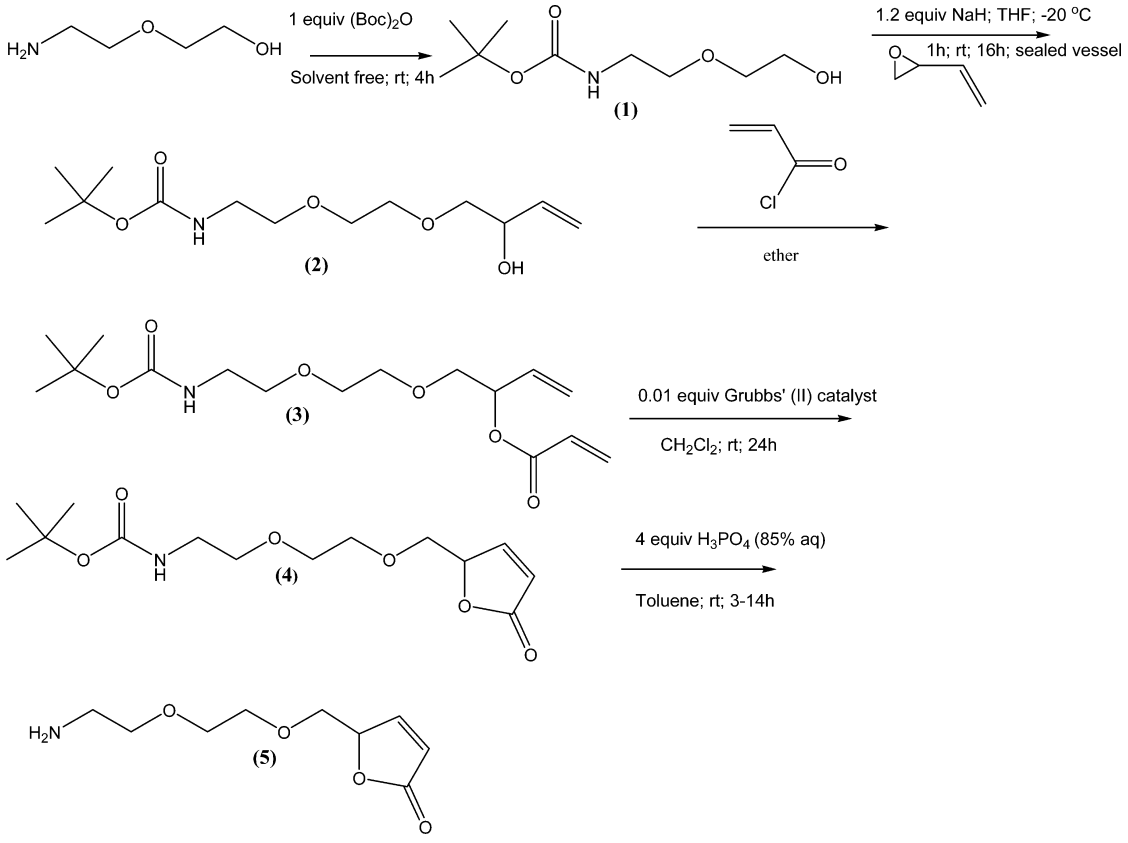

Figure 1. Synthesis of furanone 1.

inhibition. Biofilm formation on filtration membranes is one of the major limitations associated with membrane technology.[32] This reduces the quality and quantity of water in water purification systems and consequently results in higher treatment costs. To the best of the authors' knowledge, however, there have been no reports on the application of furanone-mediated QS inhibition for filtration applications. Targeting QS is also advantageous compared to the use of antibiotics since there is no risk of the bacteria developing resistance, which causes serious control problems. Many natural products contain the core 3(2*H*)-furanone structure classified as a lactone, which makes this group easily accessible.[33] Because of the high synthetic and biological importance of furanone compounds, their chemistry has received considerable attention over the past two decades.[34] In this paper, furanone derivatives were synthesized and immobilized on poly(styrene-*co*-maleic anhydride) (SMA). The furanone-modified SMA was then electrospun into nanofibers and tested for their ability to inhibit biofilm attachment.

EXPERIMENTAL METHODS

Materials. A commercial grade of SMA (M_w 110 000) containing about 28 wt % maleic anhydride as a statistical copolymer was donated by Polyscope, Geleen, The Netherlands (Grade SZ 28110). 2,5-Dimethyl-4-hydroxy-3(2H)-furanone (DMHF, 98%), butadiene monoxide (98%), acryloyl chloride, 2,2-(aminoethoxy)ethanol (98%), iodine (I_2, 99%), and sodium hydride (NaH, 95%) were obtained from Sigma Aldrich, South Africa, and used without further purification. Boc oxide ($(Boc)_2O$, 98%), Grubbs (II) catalyst (97%), sodium hydrogen carbonate ($NaHCO_3$, 99.5%), and sodium thiosulfate ($Na_2S_2O_3$, 99%) were obtained from Merck chemicals. The solvents and acids (tetrahydrofuran (THF) 99.9%, diethyl ether (98%), ethyl acetate (99.8%), triethyl amine (99.5%) dichloromethane (DCM, 99.8%), *p*-toluenesulfonic acid (98%), phosphoric acid (H_3PO_4, 95%), and toluene (99.8%)) used in this study were all purchased from Sigma Aldrich. The bacterial strains *Escherichia coli* Xen 14, *Salmonella tymphimurium* Xen 26, *P. aeruginosa* Xen 5, *Klebsiella pneumoniae* Xen 39, and *Staphylococcus aureus* Xen 36 were obtained from Caliper Life Sciences, Hopkinton MA, USA. The bacterial strains contain a *Photorhabdus luminescence luxABCDE* operon (*lux* gene) to produce the enzyme luciferase, which emits photons in the presence of ATP and oxygen.

Synthesis and Characterization of Furanone Compounds. In this study, the immobilization of furanone compounds on SMA copolymer was investigated. The importance of SMA copolymers is attributed to their usage in a number of areas for various purposes. Its applications comprise of additives that are used to upgrade properties of styrenic polymeric material, coating additives, binder application, additives for building materials, microcapsules, blend compatibilizers, adhesion promoters for polyolefin coatings on metals, and medical and pharmaceutical applications.[35−38] SMA copolymer is also regarded as a functional or reactive polymer.[39] The functionality is brought about by the maleic anhydride in the backbone of the copolymer. The maleic anhydride in the backbone of SMA is reactive toward nucleophilic reagents (H_2O, alcohols, thiols, ammonia, amines, etc). Introduction of nucleophilic compounds enables the synthesis of new materials.[40,41] SMA was chosen for these experiments because of its ease to react with amines. Two furanone compounds with dangling amines (5-(2-(2-aminoethoxy)ethoxy)methyl)-2(5H)furanone and 4-(2-(2-ami-

dx.doi.org/10.1021/bm300932u | *Biomacromolecules* 2012, 13, 3138−3150

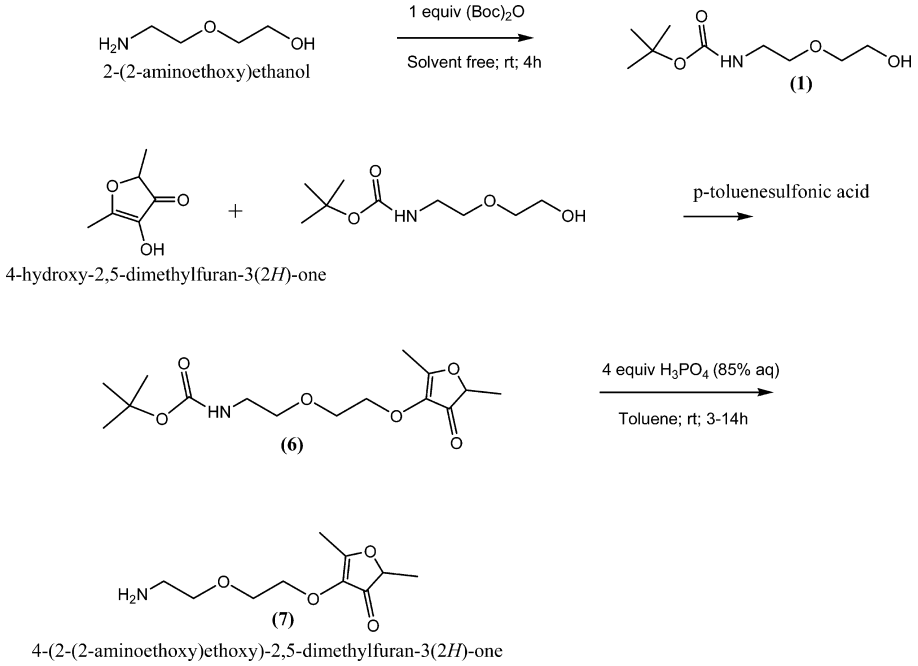

Figure 2. Synthesis of furanone 2.

noethoxy)-2,5-dimethyl-3(2H)-furanone) referred to as Furanone 1 and Furanone 2, respectively, in this paper, were synthesized in our laboratories (Figures 1 and 2). These furanones were then covalently immobilized on SMA forming furanone-modified SMA (Figure 3).

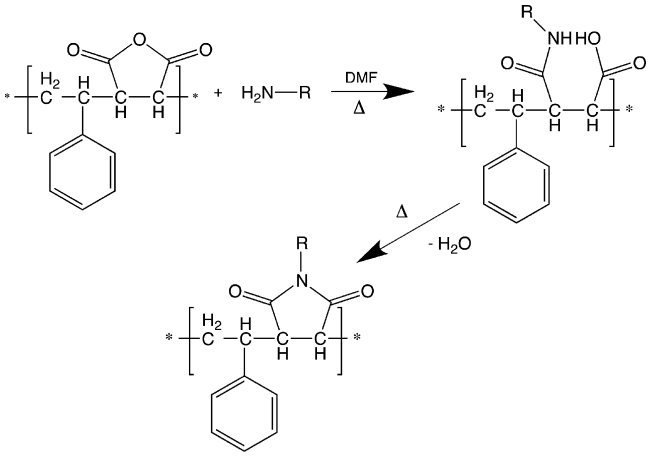

Figure 3. Immobilization of furanone derivatives on SMA copolymer backbone.[39,41].

Synthesis of furanone 1. To a magnetically stirred mixture of 2-(2-(aminoethoxy) ethanol 20.67 mL (1 mmol) and $(Boc)_2O$ 10.50 g (1 mmol), a catalytic amount of iodine 2.53 g (10 mol %) was added under solvent-free conditions at room temperature. After stirring the reaction mixture for 3 h, diethyl ether (10 mL) was added. The reaction mixture was washed with aqueous $Na_2S_2O_3$ solution (5%, 5 mL) and saturated $NaHCO_3$ solution. The organic layer was dried over Na_2SO_4, and the solvent was evaporated under reduced pressure.[42] The product was further purified using silica gel chromatography with ethyl acetate and triethylamine (7:1) as the solvent system. This step was followed by vacuum evaporation to remove any residual solvent resulting in the desired Boc-protected 2-(2-(aminoethoxy) ethanol (**1**). While stirring, 20 mL of THF was gradually added to 6.82 g of product 1 (0.036 mol) followed by 1.03 g of NaH (1.2 equiv). The reaction temperature was lowered to −20 °C using a HAAKE Thermo DC5-K75 cryostat. When the temperature reached −20 °C and the hydrogen gas had completely evolved, 2.50 g of butadiene monoxide (0.036 mol) was added to the reaction mixture and stirred for an additional 1 h. The reaction was then stirred for an additional 16 h at room temperature. Water (20 mL) was slowly added with stirring until H_2 evolution ceased. The organic layer was separated using CH_2Cl_2, washed with H_2O, and dried using 10 g Na_2SO_4 to give 6.16 g (90.32%) of **2**.[43] To alcohol **2** (6 g, 0.022 mol), 2.33 g (0.26 mol) of acryloyl chloride and 5 mL of ether were added. The mixture was then poured into water, and the organic layer was separated. Excess volatiles were removed via vacuum evaporation, and 5.88 g of product **3** (98%) was obtained. Product **3** (5.50 g, 0.017 mol) was ring-closed via metathesis by adding 3.29 g (0.01 mol) of Grubbs' second-generation catalyst, giving the Boc-protected 5-(2-(2-aminoethoxy)ethoxy)methyl)-2(5H)furanone (**4**), which after deprotection with H_3PO_4 in the presence of toluene yielded 84% product (**5**).[44] This reaction is illustrated in Figure 1. Further purification by column chromatography on silica was dismissed due to losses in product yields when these were repeatedly columned.

Synthesis of furanone 2. The amine group in 2-(2-aminoethoxy)ethanol was Boc-protected as described in the previous section, and the resultant Boc-protected product (**1**) was reacted with DMHF (2.0 g) in a 250 mL round-bottom flask in the presence of *p*-toluenesulfonic acid (100 mg) and anhydrous ethanol (80 mL). A drying tube was attached to the top of the reflux condenser, and the mixture was refluxed for 6 h. The mixture was then cooled, shaken with solid $NaHCO_3$ (5 g), and filtered through a 2 mm layer of $NaHCO_3$ to remove the acid catalyst.[45] The product contained both the starting material and the Boc-protected product, possibly because the *p*-toluenesulfonic acid deprotected the 2-(2-aminoethoxy)-

dx.doi.org/10.1021/bm300932u | *Biomacromolecules* 2012, 13, 3138−3150

ethanol. Column chromatography was used to purify the Boc-protected 4-(2-(2-aminoethoxy)-2,5-dimethyl-3(2H)-furanone. This was followed by deprotection using 4 equiv of H_3PO_4 in the presence of toluene as the solvent, giving a 78% yield (Figure 2).

Immobilization of Furanone Compounds onto SMA. In a three-necked round-bottomed flask equipped with a stirrer, 0.5 g of SMA (0.0025 mol MAnh) was placed and *N*,*N*-dimethylformamide (DMF) (20 mL) was added as a solvent. Then the solution was stirred at 70 °C. After complete dissolution of SMA, 1 g of 4-(2-(2-aminoethoxy)-2,5-dimethyl-3(2H)-furanone (0.0051 mol) was added dropwise with continuous stirring. This resulted in gelation of the reactants; vigorous stirring as well as increasing the temperature to 150 °C resulted in a clear gold solution. This solution was then dehydrated using rotary evaporation followed by vacuum evaporation to remove any residual solvents to give the final product in a yield of 91% (Figure 3). In the case of 5-(2-(2-aminoethoxy)ethoxy)methyl)-2(5H)furanone, 1.069 g of SMA (0.0051 mol MAnh) and 1.026 g of 5-(2-(2-aminoethoxy)-ethoxy)methyl)-2(5H)furanone (0.0051 mol) were used.

Nuclear Magnetic Resonance (^{1}H NMR). NMR spectroscopy was used to elucidate the chemical structures of the synthesized compounds and to determine their purity. One-dimensional ^{1}H NMR spectra were acquired with a Varian Unity Inova 600 MHz NMR spectrometer with 5 mm broadband probe at 293 K in deuterated chloroform ($CDCl_3$). Relaxation delays of 1 s and frequencies of 600 MHz were used for the ^{1}H NMR. Spectra were internally referenced to tetramethylsilane (TMS). All peaks are reported in parts per million (ppm) downfield of TMS.

Electrospray Mass Spectrometry (ES-MS). The molar masses of 5-(2-(2-aminoethoxy)ethoxy)methyl)-2(5H)-furanone and 4-(2-(2-aminoethoxy)-2,5-dimethyl-3(2H)-furanone were confirmed by ES-MS. ES-MS was carried out using a Waters API Q-TOF Ultima equipped with a Waters UPLC. The sample (3 μL) was injected at a capillary voltage of 3.5 kV, cone voltage of 35 V, and RFI value of 50. The source temperature was maintained at 80 °C, and the desolvation temperature was maintained at 350 °C. The desolvation gas was set at 350 L/h, and the cone gas was set at 50 L/h.

Attenuated Total Reflectance Fourier Transform Infrared Spectroscopy (ATR/FTIR). To confirm the immobilization of the furanone compounds onto SMA, ATR-FTIR spectroscopy was performed. A Nexus FT-IR provided by Nicolet Thermo equipped with a FTIR gas analyzer was used for ATR-FTIR studies. The spectrometer was fitted with a diamond crystal, and measurements were taken in the 600 cm^{-1} to 4000 cm^{-1} infrared-range at a resolution of 6 cm^{-1}. The spectra were based on a total of 32 scans per sample.

Size Exclusion Chromatography (SEC). Molar mass and dispersity ($Đ$) were obtained using SEC. The SEC was carried out on a dimethylacetamide (DMAc, HPLC grade) solvent system using a flow rate of 1.0 mL/min. The instrument setup consisted of a Shimadzu LC-10AD pump, a Waters 717 plus autosampler, a column system fitted with a 50 × 8 mm guard column in series with three 300 × 8 mm, 10 μm particle size GRAM columns (2 × 3000 Å and 100 Å) obtained from PSS, a Waters 2487 dual wavelength UV detector and a Waters 410 differential refractive index (DRI) detector all in series. 100 μL injection volumes were used, and the oven temperature of the column and DRI detector was kept at 40 °C. The solvent was stabilized with 0.05% butylhydroxytoluene (BHT) (w/v) and 0.03% LiCl (w/v), and samples were filtered through a 0.45 μm GH Polypro (GHP) filter to prevent any impurities from entering the system. Calibration was performed on poly(methyl metachrylate) (PMMA) standards (Polymer Laboratories) ranging from 690 to 1.2 × 10^6 g/mol. Data acquisition was done using Millennium[32] software, version 4.

Electrospinning. The modified polymers (SMA/5-(2-(2-aminoethoxy)ethoxy)methyl)-2(5H)furanone (SMA/Furanone 1) and SMA/4-(2-(2-aminoethoxy)-2,5-dimethyl-3(2H)-furanone (SMA/Furanone 2)) were dissolved in (1:1) mixtures of ethanol and methanol to form 10 wt %/vol electrospinning solutions. Pristine SMA dissolved in THF was used for control experiments. Bubble electrospinning, which is described in detail by Gule and co-workers was used for nanofiber production.[46] All the polymer solutions were electrospun at room temperature. The widget-collector distance used was 20 cm and the relative humidity was maintained between 45 and 60% for continuous fiber formation. The applied voltage used was between 45 and 50 kV. The nanofibrous mats were cross-linked by heat treatment at 120 °C for 15 min.

Scanning Electron Microscopy (SEM). The morphology of the nanofibers was observed with SEM. Analyses were performed on a Leo 1430VP coupled with a Cambridge S200 scanning electron microscope after gold sputter coating was applied. The conditions for image acquisition were an accelerating voltage of 7 kV and a probe current of 150 pA for the former and an accelerating voltage of 10 kV and a probe current of 50 pA for the latter. For determination of fiber diameters the SEM_Img_Studio software, which runs using the National Instruments LVRunTime Engine, version 1.1.0, was used.

To measure the fiber diameters, the electrospun nanofibrous mats were viewed under the SEM at a magnification between 1000 and 5000×. This magnification range was chosen such that up to 50 fibers were included in the image. Each image was then processed using SEM_Img_Studio Software. A minimum of 15 measurements were taken, and the highest and lowest values were discarded prior to calculating the average. Solvent beaded and clumped fibers were considered outliers and therefore were not included in the measurements. The porosity of nanofibrous mats is another very important parameter, especially since it determines the air and water permeability through the fiber mat.[47] To measure pore sizes, area light intensity scans were performed using the Scanning Probe Image Processor (SPIP) Image Metrology A/S, version 5.1.3 software. This software uses SEM images to calculate fiber mat porosity.

Antimicrobial Inhibition. To determine the antimicrobial efficiency of the nanofibers, the basic plate counting technique was adopted. These tests were confirmed with bioluminescent imaging (BLI) and LIVE/DEAD BacLight to determine the antimicrobial efficiency against viable but nonculturable (VBNC) cells. This was done to quantify the cells that enter a dormant state during contact with the antimicrobial fibers and to eliminate the chances of overestimating the antimicrobial efficiency of the nanofibers. The electrospun nanofibers were supported on 0.22 μm sized Millipore filter membranes for antimicrobial tests and without a support for cell adhesion-inhibition tests. For each of the tests, the amount of nanofibers was 10 mg.

Plate counts. *K. pneumoniae* Xen 39, *S. aureus* Xen 36, *E. coli* Xen 14, *P. aeruginosa* Xen 5, and *S. typhimurium* Xen 26 were used to test the antimicrobial and cell-adhesion inhibition

properties of the modified polymers. Each pathogen was cultured in 10 mL brain heart infusion (BHI) broth (Biolab Diagnostics) along with the appropriate antibiotics overnight on a rotating wheel at 37 °C. For each strain, cells were pelleted by 10 min centrifugation at 3000 rpm, and washed three times with physiological water. The optical densities (ODs) were measured using a Biorad smart spec plus spectrophotometer. Spiked water samples were prepared by inoculating 1×10^{10} CFU/mL (1 mL) of each strain into 500 mL sterile physiological water. Several control (cell viability) experiments (not reported here) were carried out to verify the absence of osmotic lysing, which often occurs when cells (especially gram negative) are removed from rich media into physiological water.[48,49] The spiked water was then filtered through pristine SMA (control) or furanone-modified nanofibrous mats. The nanofibers were then rinsed several times using 10 mL physiological water to wash off all remaining bacterial cells and the wash-off water was plated out on BHI agar plates to determine living cells. After washings, the membranes were viewed under the XENOGEN VIVO VISION In Vivo Imaging Lumina System (IVIS) to ascertain complete removal of the cells. Other techniques such as vortexing of the membranes in physiological water to remove all cells that may be trapped inside the membrane were also investigated and yielded similar results. This was done after specific contact periods to determine cell death as a function of time. After incubation of the plates overnight at 37 °C, colony counting was used to determine the antimicrobial effect of the filters. The experiment was performed for each pathogen and each specific contact period in triplicate. In order to mimic a real-life scenario where bacteria species coexist, 20 μL of each pathogen from the 10^6 CFU/mL stock was inoculated into the same tube containing 10 mL BHI broth to make a cocktail of the strains, and antimicrobial tests were conducted as described previously.

Cell-Adhesion Inhibition Characterization. The cell-adhesion inhibition capacity of the furanone-modified nanofibrous mats was carried out. To do this, a method similar to the one used by Alvarez and co-workers was modified and used for our experiments.[50] Weighed (10 mg) furanone-modified nanofibrous mats were immersed in BHI (10 mL) media containing *E. coli* Xen 14, *S. tymphimurium* Xen 26, *P. aeruginosa* Xen 5, *K. pneumoniae* Xen 39, and *S. aureus* Xen 36. For each of the strains, attachment inhibition was monitored after culturing at different time intervals (0–36 h) as illustrated in Figure 4. At each of these time intervals, the nanofibrous mats were removed from the culture media and rinsed in physiological water to remove unattached colonies. These were then either rinsed with physiological buffered saline (PBS) or vortexed prior to plating out. For imaging, the mats were rinsed and stained prior to fluorescence imaging. Real biofilm development and biofilm architecture were not studied, and future studies on these nanofibers will explore these details.

BLI. BLI is a relatively new development, which uses the light emitted from genetically modified living organisms as a tool for molecular imaging in small laboratory animals. It has been used by other researchers and has been found to offer a method that is sensitive and innocuous and only allows live or viable cells to be detected.[51−53] This technique measures cell viability by quantifying total photons emitted by the cells. In order to apply the BLI system in the antimicrobial evaluation, engineered bacterial strains obtained from Caliper Life Sciences (Hopkinton MA, USA) were used for the assessment in this study. The bacterial strains have a *Photorhabdus luminescence*

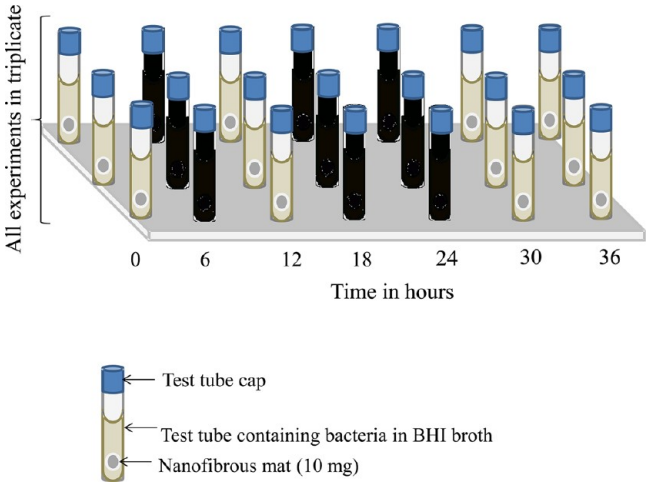

Figure 4. Cell adhesion inhibition characterization setup.

luxABCDE operon (*lux* gene) to produce the enzyme luciferase, which emits photons in the presence of ATP and oxygen. These photons indicate metabolic activity in the pathogens. Research on BLI corresponded with plate counting data with a correlation efficiency of about 0.98.[54] After filtration of the spiked samples (as described in the Plate Counts section) the nanofibrous mats were placed in a XENOGEN VIVO VISION In Vivo Imaging Lumina System (IVIS) supplied by Caliper Life Science, and the Living Image 3.1 Software was used to process them. Imaging was performed immediately after filtering the spiked water through the furanone-modified nanofibrouos mats and also after 10 min exposure to monitor the level of bioluminescence emitted by the strains.

Fluorescence Experiments. Furanone-modified and control nanofibrous mats (10 mg) were exposed to the pathogen cocktail (1×10^{10} cells) described in the Plate Counts section along with the appropriate antibiotics [*E. coli* Xen 14 (Kanamycin, 30 μg/mL), *S. tymphimurium* Xen 26 (Kanamycin, 30 μg/mL), *P. aeruginosa* Xen 5 (Tetracycline, 60 μg/mL), *K. pneumoniae* Xen 39 (Kanamycin, 200 μg/mL), and *S. aureus* Xen 36 (Kanamycin, 30 μg/mL)] overnight on a rotating wheel at 37 °C. These mats were then taken out of the media using forceps and rinsed lightly using physiological water. LIVE/DEAD BacLight kit with SYTO 9 and propidium iodide fluorescent dyes purchased from Molecular Probes, Inc. were used to stain the specimen for imaging purposes. SYTO 9 stains all cells green, while propidium iodide penetrates cells whose cell membrane has been damaged and stains them red. Viable and total counts can be obtained in one staining step. Staining was done by incubation of samples with 6.5 μM dye at room temperature for 10 min. These samples were then observed on an Olympus Cell-R system attached to an IX-81 inverted fluorescence microscope equipped with a F-view-II cooled CCD camera (Soft Imaging Systems). Using a Xenon-Arc burner (Olympus Biosystems GMBH) as light source, images were excited with the 472 or 572 nm excitation filter. Emission was collected using a UBG triple-band-pass emission filter cube. For the image frame acquisition, an Olympus Plan Apo N 60x/1.4 Oil objective and the Cell-R imaging software were used. Images were processed and background-subtracted using the Cell-R software.

Gas Chromatograph-Coupled Mass Spectroscopy (GC-MS). The leaching of chemical compounds into the

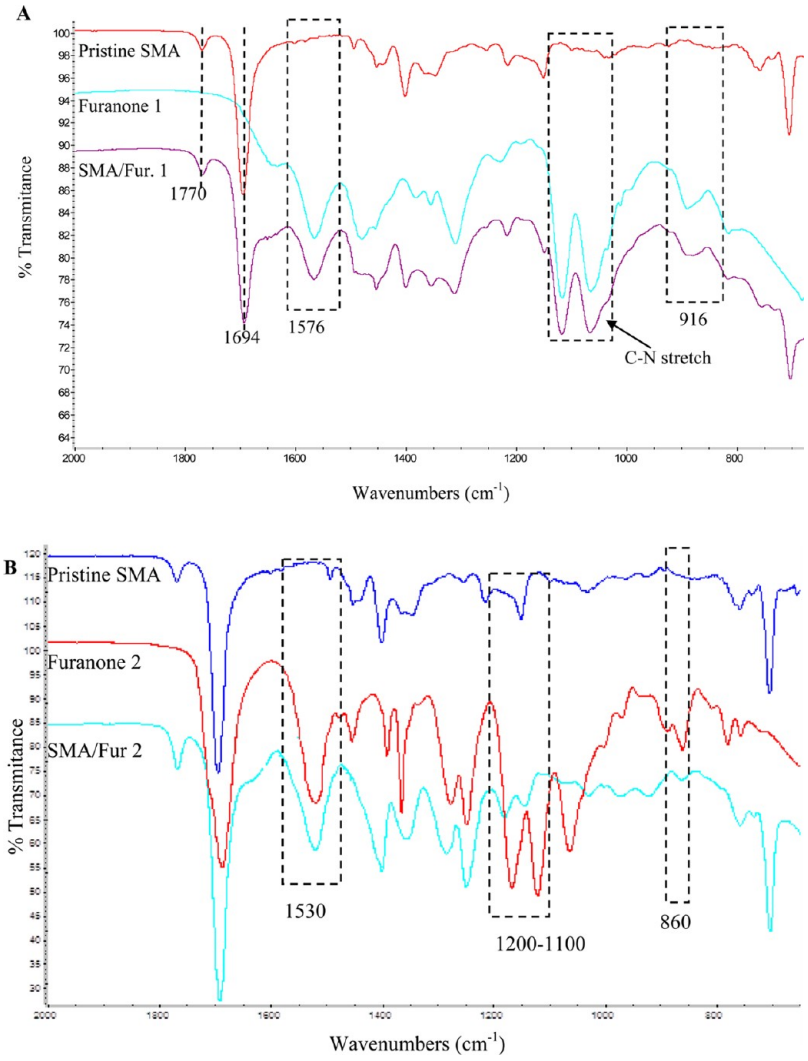

Figure 5. Overlaid ATR-FTIR of SMA and SMA/Furanone 1 showing the conversion of SMA into SMA/Furanone 1 (A) and SMA/Furanone 2 (B).

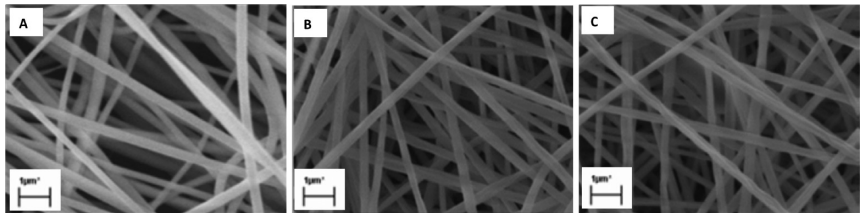

Figure 6. Morphology of electrospun neat SMA (A), SMA/Furanone 1 (B), and SMA/Furanone 2 nanofibers.

environment is often accompanied by health and pollution concerns. To determine whether the furanone derivatives did not leach into filtered water, water filtered through the nanofibrous mats was screened for traces of furanones using GC-MS. As a positive control, distilled water spiked with 0.02 M 5-(2-(2-aminoethoxy)ethoxy)methyl)-2(5H)furanone (furanone 1) was analyzed, and distilled water was used as a negative control. GC-MS was performed using a Waters GCT spectrometer equipped with CTC CombiPAL Autosampler, and a DB XLB column (30 m, 0.25 mm ID, 0.1 μm film thickness) was utilized. Solid phase microextraction (SPME) vials were used in the analysis, and the headspace of the samples were analyzed using a CTC PAL auto sampler.

RESULTS AND DISCUSSION

^{1}H NMR. ^{1}H NMR was used to confirm the structures of the synthesized 5-(2-(2-aminoethoxy)ethoxy)methyl)-2(5H)-furanone and 4-(2-(2-aminoethoxy)-2,5-dimethyl-3(2H)-furanone. All the peaks are reported in ppm downfield of TMS. Furanone 1: (^{1}H NMR: 600 MHz, $CDCl_3$ δ = 3.42 (m, 2H), 3.58 (m, 5H), 3.81 (m,2H), 4.42 (s,2H), 4.98 (m,1H), 5.35 (*m* = 1H), 6.32 (*s* = 2H)). Furanone 2: (^{1}H NMR: 600 MHz, $CDCl_3$ δ =1.22 (s,3H), 2.16 (s,3H), 2.98 (m,2H), 3.32 (m, 4H), 3.62 (m,2H), 3.74 (m.1H), 6.67(s,2H)). These results confirmed the structures of the furanone compounds.

ES-MS. ES-MS spectra confirmed the molar masses of 5-(2-(2-aminoethoxy)ethoxy)methyl)-2(5H)furanone and 4-(2-(2-

dx.doi.org/10.1021/bm300932u | *Biomacromolecules* 2012, 13, 3138−3150

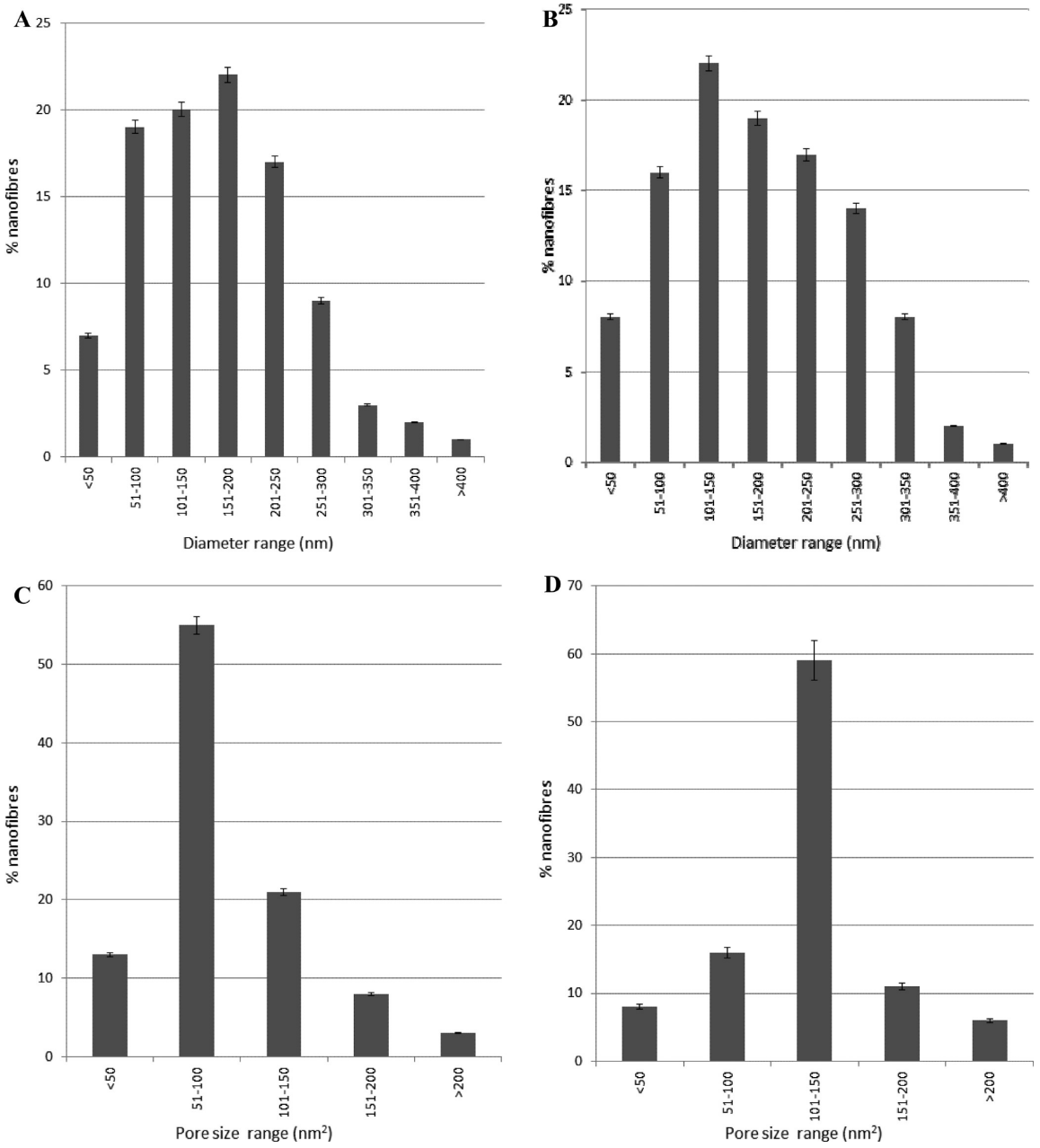

Figure 7. Nanofiber diameters of SMA/Furanone 1 (A) and of SMA/Furanone 2 (B) and pore sizes of SMA/Furanone 1 (C) and of SMA/Furanone 2 (D) nanofiber mats.

Table 1. Summary of Antimicrobial and Cell Adhesion-Inhibition Achieved by the Synthesized Furanones

		P. aeruginosa Xen 5	*E. coli* Xen 14	*S. typhimurium* Xen 26	*S. aureus* Xen 36	*K. pneumoniae* Xen 39
antimicrobial efficacy after 30 min (log CFU/mL reduction)	SMA nanofibers	0	0	0	0	0
	neat furanone 1	2.68	2.79	2.01	1.35	2.23
	neat furanone 2	3.45	3.62	3.09	3.76	3.66
	SMA/Furanone 1 nanofibers	1.12	0.79	0.8	0.83	0.6
	SMA/Furanone 2 nanofibers	3.78	2.62	3.26	3.02	2.66
cell adhesion-inhibition after 36 h (log CFU/mL reduction)	SMA nanofibers	0	0	0	0	0
	neat furanone 1	2.38	2.49	1.51	1.75	2.02
	neat furanone 2	4.68	4.67	3.79	4.66	3.66
	SMA/Furanone 1 nanofibers	1.88	1.21	2.03	1.35	2.23
	SMA/Furanone 2 nanofibers	3.22	4.22	1.79	3.66	3.66

dx.doi.org/10.1021/bm300932u | *Biomacromolecules* 2012, 13, 3138−3150

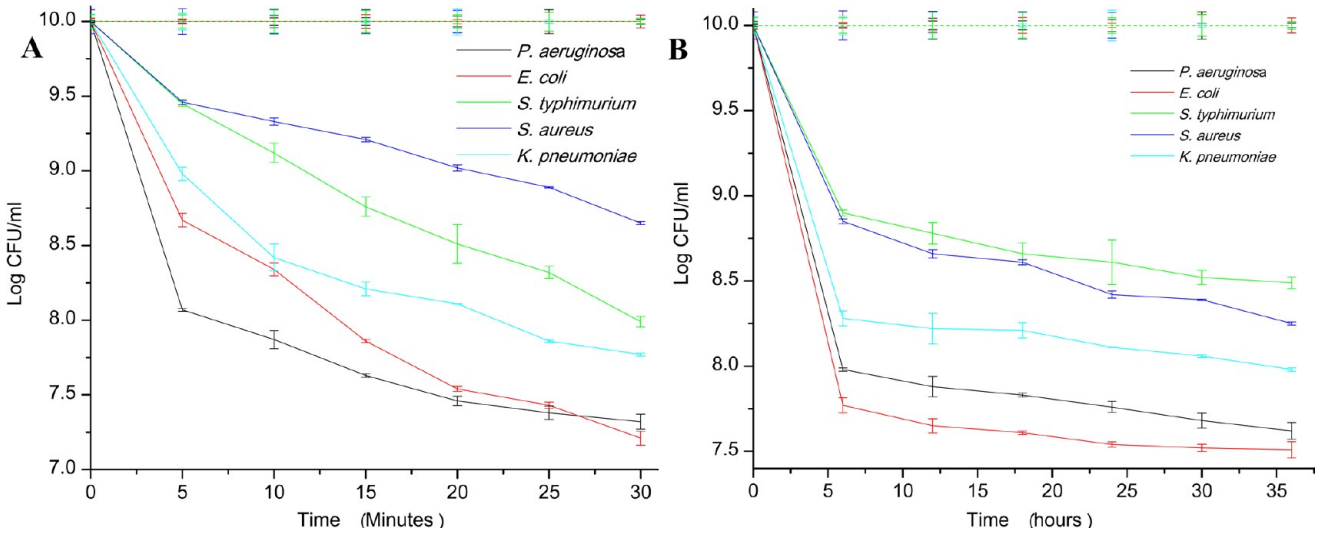

Figure 8. Antimicrobial (A) and antifouling (B) potential of neat furanone 1 over 30 min and 36 h respectively.

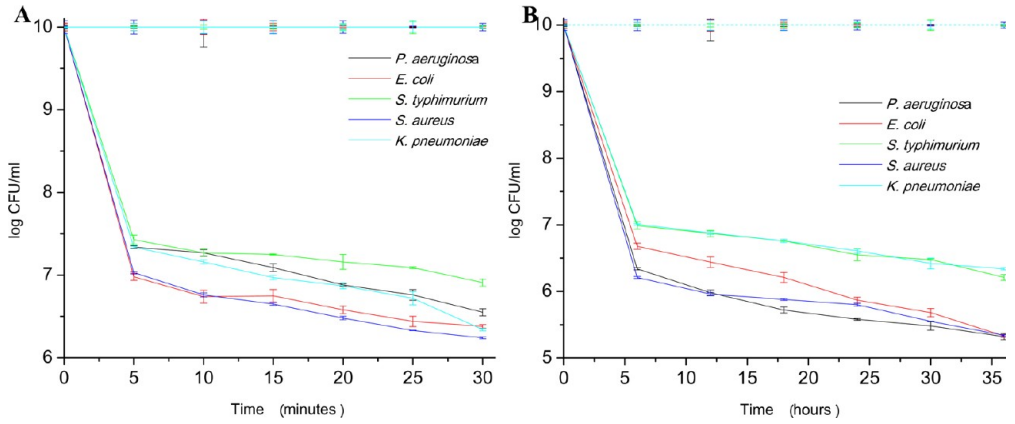

Figure 9. Antimicrobial (A) and antifouling (B) potential of neat furanone 2 over 30 min and 36 h, respectively.

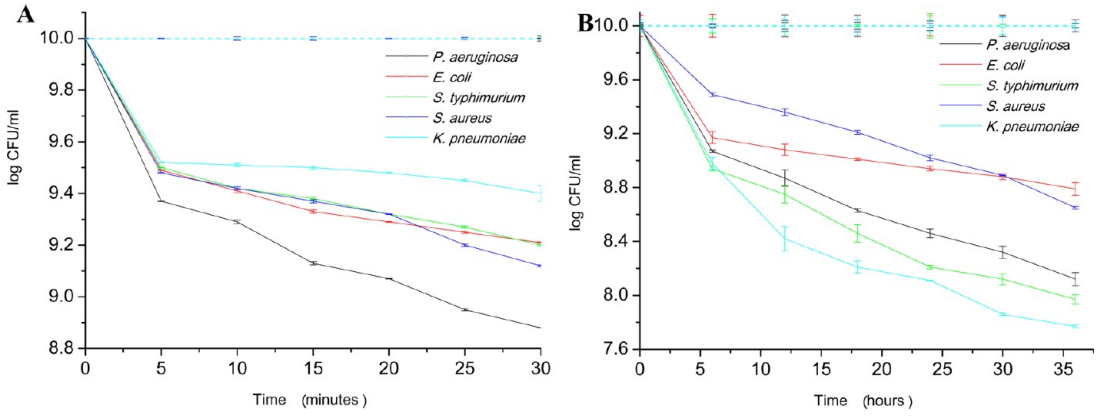

Figure 10. Antimicrobial (A) and cell-adhesion inhibition (B) potential of SMA/Furanone 1 nanofibrous mats over 30 min and 36 h, respectively.

aminoethoxy)-2,5-dimethyl-3(2H)-furanone to be m/z 215.01 and m/z 201.1, respectively. This corresponds to calculated molar masses of 215.101 g for 5-(2-(2-aminoethoxy)ethoxy)-methyl)-2(5H)furanone and 201.110 g for 4-(2-(2-aminoethoxy)-2,5-dimethyl-3(2H)-furanone.

ATR/FTIR Spectroscopy. ATR/FTIR spectroscopy was used to confirm successful immobilization of the furanone moiety on SMA. Figure 5A,B compares the ATR/FTIR spectra of pristine SMA with that of the synthesized furanones and SMA modified with furanones. The absorption peak at 1185 cm^{-1} is characteristic of the amide stretch.[55] The imide groups around 1694 cm^{-1} are characteristic of the asymmetric and symmetric C═O stretching vibrations. The signals at 1576 cm^{-1} and around 1500 cm^{-1} are caused by (C═C) stretching of the aromatic ring and (C−H) bending vibration of the aromatic ring, respectively. The band at 916 cm^{-1} is due to cyclic anhydride groups. From the highlighted similarities on the spectra (Figure 5A and 5B), the incorporation of the

dx.doi.org/10.1021/bm300932u | Biomacromolecules 2012, 13, 3138−3150

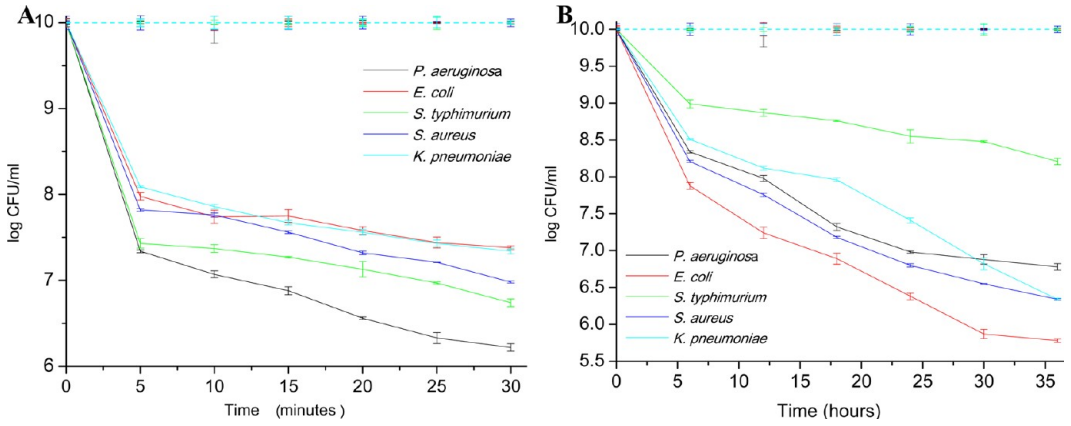

Figure 11. Antimicrobial (A) and cell-adhesion inhibition (B) potential of SMA/Furanone 2 nanofibrous mats over 30 min and 36 h, respectively.

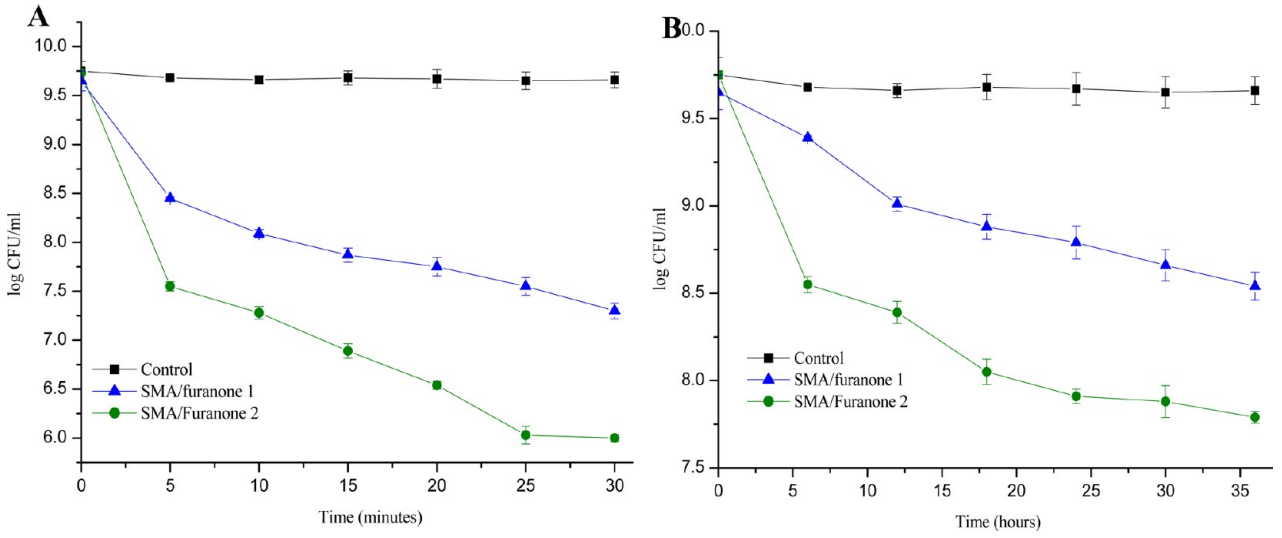

Figure 12. Antimicrobial (A) and attachment-inhibition (B) potential of nanofibrous mats on mixed strains.

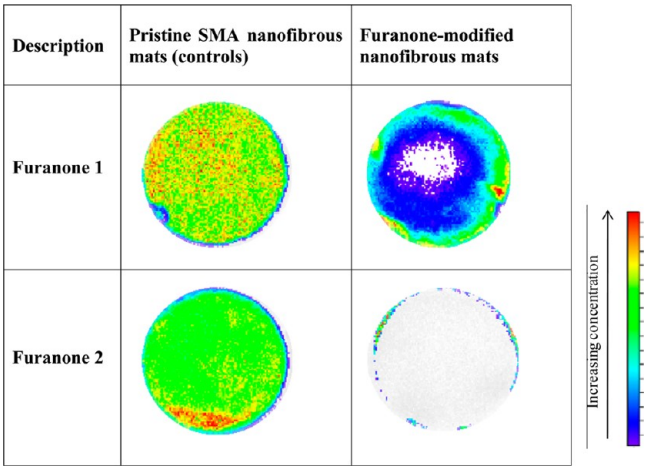

Figure 13. In vivo images illustrating the antimicrobial efficacy of the furanone-modified nanofibrous mats after 10 min of exposure of a mixed culture.

furanone moiety onto the SMA backbone is clearly demonstrated.

Conversion Efficiency of SMA to SMA/Furanone. After immobilization of the furanone compounds on SMA, both furanone-containing polymers were dissolved in methanol to precipitate out any residual SMA. There was no precipitate, which indicated that there was no excess SMA present in the furanone-modified SMA. This gave a good indication that complete conversion of SMA to SMA/Furanone had taken place. The furanone containing SMA was rotary evaporated and dried in a vacuum pump to remove the methanol, and the yields remained consistent to further confirm that none of the SMA was precipitated. SEC of the polymer was consistent with the polymer, with a molar mass (M_n) of 112 000 and dispersity ($Đ$) of 2.7 for SMA/Furanone 1. For SMA furanone 2, M_n was 111 900, and the dispersity ($Đ$) was 2.3.

Morphology of the nanofibers. The morphology of both SMA/Furanone 1 and SMA/Furanone 2 nanofibers did not differ much from that of neat SMA (Figure 6A–C). The fibers exhibited smooth morphology with no solvent beading. Individual fibers in these mats had diameters averaging between 120 and 220 nm (Figure 7A,B). Although there is no specific diameter range for nanofibrous materials in filter applications, according to the filtration theory, smaller fiber diameters give better filtration efficiency.[56] This is because thinner fibers result in high surface-to-volume ratios, which are advantageous for filtration application. This was a good property since it increased the surface area for water filtration. These nanofibrous mats also had average pore sizes of less than 120 nm[2] (Figure 7C,D). The sizes of the mat pores are very important

dx.doi.org/10.1021/bm300932u | Biomacromolecules 2012, 13, 3138–3150

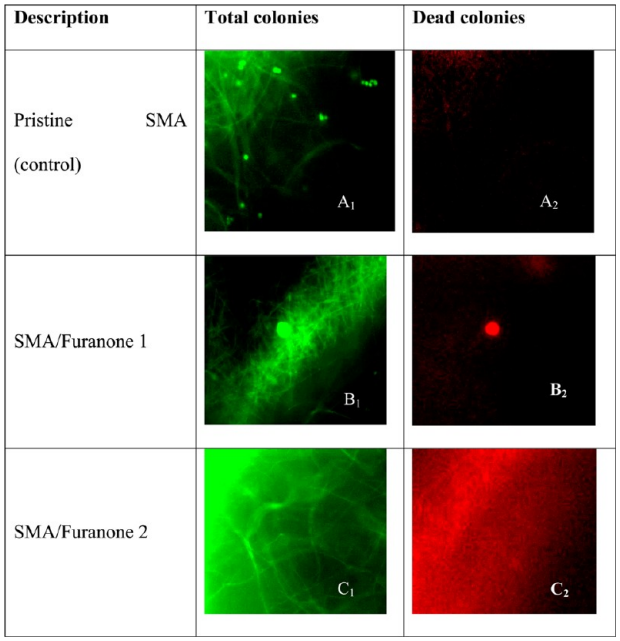

Figure 14. Fluorescence microscopy images showing cell-adhesion inhibition and antimicrobial efficacy of the furanone-modified nanofibrous mats.

for this study since, for accuracy in measuring antimicrobial efficacy, the pores have to be smaller than the sizes of the studied bacteria strains. The recorded pore sizes were all less than 250 nm^2 and therefore appropriate for further tests.

Antimicrobial and Cell-Adhesion Inhibition Characterization. A lot of research has been done on furanone compounds with both 2(5H) and 3(2H) cores. Free furanone derivatives with 2(5H) cores have demonstrated antimicrobial activity against bacterial strains and even fungi.[22,57−62] In zone inhibition tests, 4-amino-5-hydroxy-2(5H)-furanones demonstrated an average of 10 mm inhibition of *E. coli*, *S. aureus*, *P. aeruginosa*, *K. pneumoniae* and *Enterobacter spp.*[57] Work done by Lönn-Stenstud and co-workers also showed that this class of furanone compounds significantly reduced *P. aeruginosa* lung infection in mice.[58] Even though these studies did not use similar techniques to quantify antimicrobial and cell-adhesion inhibition efficiencies, they showed convincingly that furanone derivatives with 2(5H) cores had antimicrobial properties.

The antimicrobial efficiency of synthetic and natural furanone derivatives with the 3(2H) core has also received vast interest among researchers.[46,63−65] One of the most interesting reports was published by Kataoka, where he investigated the composition of Japanese soy sauce, which among other properties has been found to be antimicrobial and anticarcinogenic. This sauce was found to contain 4-hydroxy-2(or 5)-ethyl-5(or 2)-methyl-3(2H)-furanone (HEMF), DMHF, and 4-hydroxy-5-methyl-3(2H)-furanone (HMF). This sauce has demonstrated up to 3 log reduction of strains *S. aureus*, *Shigella spp.*, *Vibrio cholera*, *Salmonella spp.*, and *E. coli* within 4−6 h of contact.[66] A similar study also demonstrated up to 4.5 log reductions in populations of *K. pneumoniae* Xen 39, *S. aureus* Xen 36, *E. coli* Xen 14, *P. aeruginosa* Xen 5, and *S. typhimurium* Xen 26.[46] Sung and co-workers also reported exceptional antimicrobial efficacy of DMHF toward strains of *P. aeruginosa*, *S. aureus*, *E. coli*, and Enterococci.[63]

In the present study, as summarized in Table 1, the neat furanones as well as SMA-immobilized furanones showed good antimicrobial and cell adhesion-inhibition properties. In both cases (neat and immobilized), furanone 2 showed greater activity than furanone 1. To fully understand this phenomenon would require further insight into the biochemical QS pathway taken by these furanone compounds specifically. Neat furanone 1 reduced populations of *P. aeruginosa* Xen 5, *E. coli* Xen 14, *S. typhimurium* Xen 26, *S. aureus* Xen 36, and *K. pneumoniae* Xen 39 by an average of 1.5 log after 30 min (Figure 8A). *P. aeruginosa* Xen 5 was reduced more than all the other strains by 2.7 log, and *S. aureus* Xen 36 was the least reduced by 1.4 log. The free furanone also inhibited attachment by more than 1.5 log for all of the studied strains after 36 h (Figure 8B). SMA/Furanone 1 nanofibers on the other hand exhibited lower antimicrobial efficiency (up to 1.1 log reduction of *P. aeruginosa* Xen 5) after 30 min exposure (Figure 10 A). Adhesion-inhibition of more than 1.2 log was achieved for all strains after 36 h (Figure 10 B).

The antimicrobial activity of neat furanone 2 was more than 3 log for all the strains tested (Figure 9A). The furanone compound also showed more than 4.5 log cell adhesion-inhibition of *P. aeruginosa* Xen 5, *E. coli* Xen 14, and *S. aureus* Xen 36. *S. typhimurium* Xen 26 and *K. pneumoniae* Xen 39 were also inhibited by more than 3.6 log after 36 h (Figure 9B). Nanofibrous mats made from SMA/Furanone 2 showed up to 3.8 log reductions in populations of *P. aeruginosa* Xen 5, closely followed by *S. typhimurium* Xen 26, which was reduced by up to 3.3 log after 30 min of exposure (Figure 11A). *E. coli* Xen 14, *S. aureus* Xen 36, and *K. pneumoniae* Xen 39 were all reduced by at least 2.6 log after 30 min of exposure. The SMA/Furanone 2 nanofibers also inhibited cell-adhesion by more than 3 log for all the strains except *S. typhimurium* Xen 26 over 36 h of exposure (Figure 11B).

The cultured mixed strains (Figure 12 A) were also significantly reduced by the furanone-modified nanofibers, and a similar trend was observed where the furanone 2-modified polymer nanofibrous mats showed higher potency than the furanone 1-modified polymer nanofibrous mats. The slightly higher activity in the mixed strains could be due to competition stresses for nutrients, which were already being experienced by the strains especially after 36 h of incubation. This is, however, not significant enough to draw any concrete conclusions.

BLI. In vivo imaging of nanofibrous mats after exposure to a mixed strain culture of *P. aeruginosa* Xen 5, *E. coli* Xen 14, *S. typhimurium* Xen 26, *S. aureus* Xen 36, and *K. pneumoniae* Xen 39 was carried out to confirm the results obtained from plate counting. Metabolically active (viable) bacterial cells show bioluminescence as indicated in Figure 13. The degree of bioluminescence changes with increase in concentration as illustrated by the scale in Figure 13. From these results, the antimicrobial nature of the furanone compounds is clearly demonstrated. The mats made from SMA/Furanone 2 still demonstrated high antimicrobial potential compared to those made from SMA/Furanone 1.

Fluorescence Microscopy. In Figure 14, the fluorescence microscopy results after staining for live/dead cells are shown. The green dye (SYTO 9) stains all bacteria colonies on the mats and the red dye (propidium iodide) stains cells with ruptured membranes (dead cells). The fibers also absorbed some of the dyes, and bacteria colonies can be differentiated from the fibers because they appear as distinct dots on the nanofiber surfaces. The control SMA images in Figure 14A did not have antimicrobial activity. This is indicated by the fact that

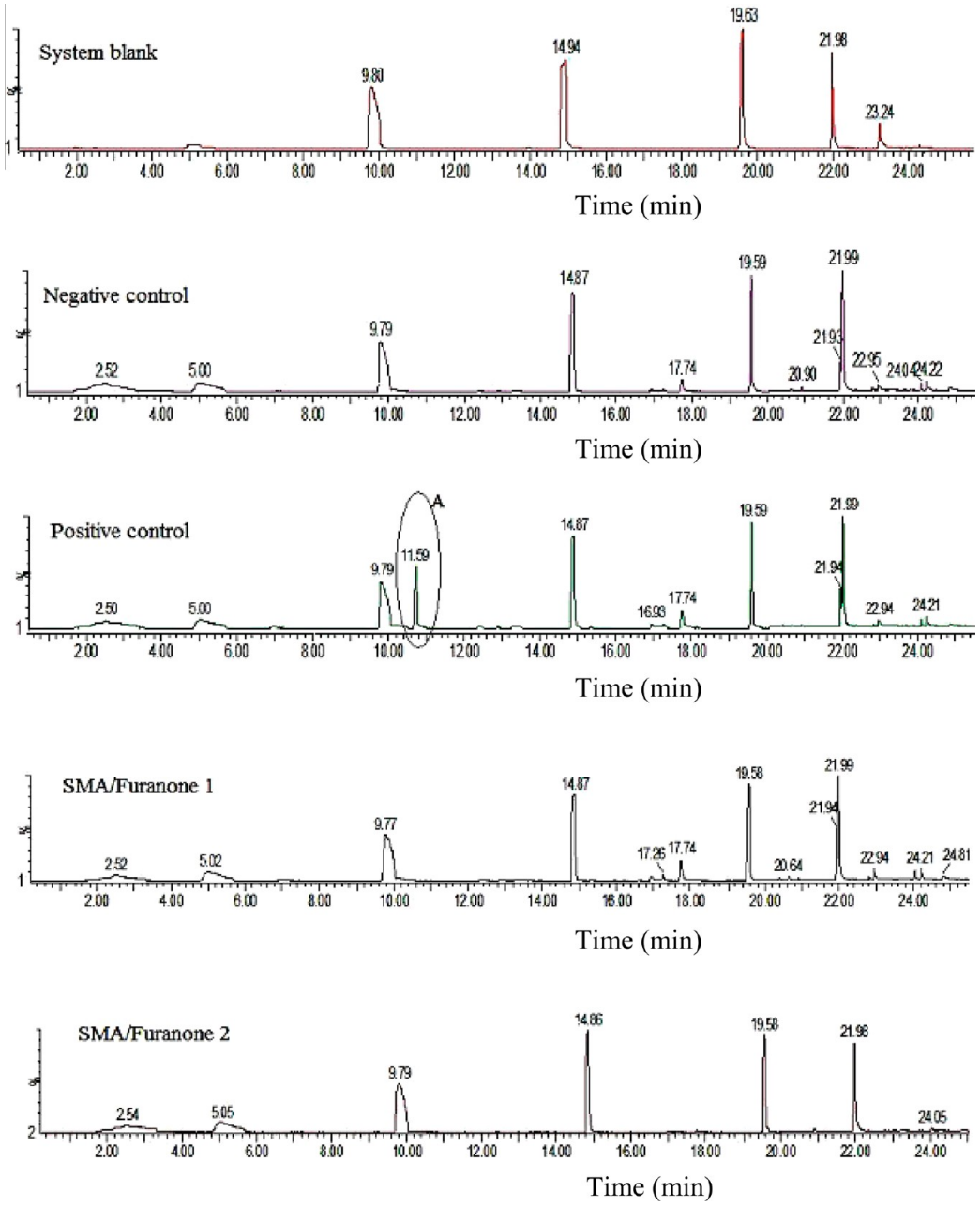

Figure 15. GC-MS spectra indicating that furanone compounds did not leach from nanofibrous mats into the filtered water.

none of the available (Figure 14A_1) bacteria colonies were dead (they did not absorb propidium iodide; Figure 14A_2). These nanofibers also did not inhibit attachment as indicated by the attached colonies (Figure 14A_1). Furanone-modified nanofibers, on the other hand, demonstrated inhibition of cell adhesion in that no colonization was visible (Figure 14B,C). These results also confirmed cell deactivation (antimicrobial activity), and this is indicated by the colony, which managed to attach to the nanofibers, but was deactivated (absorbed the red dye indicating cell death) (Figure 14 B_2).

Leaching. GC-MS experiments were carried out to investigate the leaching of the furanone derivatives from the fibers. As expected for covalently bound compounds, the GC-MS results indicated that the furanone compounds did not leach into the filtered water. The characteristic signal observed at 11.59 min in the positive control (spiked with the furanone-derivative) was absent in all the leaching experiments (Figure 15).

■ CONCLUSIONS

The syntheses of 5-(2-(2-aminoethoxy)ethoxy)methyl)-2(5H)-furanone and 4-(2-(2-aminoethoxy)-2,5-dimethyl-3(2H)-furanone were successfully carried out. The structures and molar masses were confirmed using ^{1}H NMR and ES mass spectrometry. Both furanone derivatives were successfully immobilized onto the SMA copolymer. The furanone-modified SMA was electrospun to obtain nanofibers. The nanofibrous mats demonstrated good antimicrobial and cell-adhesion inhibition efficiency against *P. aeruginosa* Xen 5, *E. coli* Xen 14, *S. typhimurium* Xen 26, *S. aureus* Xen 36, and *K. pneumoniae* Xen 39 individually and in mixed cell culture form. The 3(2H) furanone had high activity compared to the 2(5H) furanone. It

dx.doi.org/10.1021/bm300932u | *Biomacromolecules* 2012, 13, 3138−3150

is, however, not clear why the 3(2H) furanone has a higher activity compared to the 2(5H) furanone; structural differences between the two furanone compounds may be attributed to this, because the same number of moles of the furanone compounds was used in the SMA modifications. Further biochemical studies need to be done for proper understanding of the QS pathways taken by the furanone compounds to inhibit cell attachment-inhibition and antimicrobial properties of these furanones.

AUTHOR INFORMATION

Notes

The authors declare no competing financial interest.

ACKNOWLEDGMENTS

The authors would like to acknowledge the University of Stellenbosch, the Andrew Mellon Foundation, Eskom and the South African Research Chairs Initiative (SARChI) from the Department of Science and Technology (DST), and the National Research Foundation (NRF) for funding this project.

REFERENCES

(1) Chen, X.; Stewart, P. S. *Environ. Sci. Technol.* **1996**, *30*, 2078−2083.
(2) Kramer, J. F. *Biofilm control with bromo-chloro-dimethylhydantoin*; Paper number 1277; NACE International: Houston, TX, 2001.
(3) Vidella, H. A. *Int. Biodeterior. Biodegrad.* **2002**, *49*, 259−270.
(4) Stewart, P.; Roe, F.; Rayner, J.; Elkins, F. G.; Lewandowski, Z.; Ochsner, U. A.; Hassett, D. J. *Appl. Environ. Microbiol.* **2000**, *66*, 836−838.
(5) Presterl, E.; Suchomel, M.; Eder, M.; Reichmann, S.; Lassnigg, A.; Graninger, W.; Rotter, M. *J. Antimicrob. Chemother.* **2007**, *60*, 417−420.
(6) Richards, M. Self immobilization of single and combinations of enzymes in spherical particles and evaluation of their anti-biofouling potential. Masters Dissertation, University of Pretoria, Pretoria, South Africa, 2010.
(7) Meyer, B. *Int. Biodeterior. Biodegrad.* **2003**, *51*, 249−253.
(8) Allison, D. G.; Ruiz, B.; SanJose, C.; Jaspe, A.; Gilbert, P. *FEMS Microbiol. Lett.* **1998**, *167*, 179−184.
(9) Van der Borden, A. J.; Van der Mei, H. C.; Busscher, H. J. *J. Biomed .Mater. Res.* **2004**, *68B*, 160−164.
(10) Curtin, J. J.; Donlan, R. M. *Antimicrob. Agents Chemother.* **2006**, *50*, 1268−1275.
(11) Al-Sha'alan, N. *Molecules* **2007**, *12*, 1080−1091.
(12) Revanasiddappa, H. D.; Vijaya, B.; Kumar, S.,L.; Prasad, K.,S. *World J. Chem.* **2010**, *5*, 18−25.
(13) Zhuang, X.; Cheng, B.; Kanga, W.; Xua, X. *Carbohydr. Polym.* **2010**, *82*, 524−527.
(14) Muñoz-Bonilla, A.; Fernández- Garćia, M. *Prog. Polym. Sci.* **2012**, *37*, 281−339.
(15) Gottesdiener, K.; Mehlisch, D. R.; Huntington, M; Yuan, W.; Brouwn, P.; Gertz, B.; Mills, S. *Clin. Ther.* **1999**, *21*, 1301−1312.
(16) Baveja, J. K.; Li, G.; Nordon, R. E.; Hume, E. B. H.; Kumar, N.; Willcox, M. D. P.; Poole-Warren, L. A. *Biomaterials* **2004**, *25*, 5013−5021.
(17) Lattmann, E.; Ayuko, W.,O.; Kinchinaton, D.; Langley, C. A.; Singh, H.; Tisdale, M.,J. *J. Pharm. Pharmacol.* **2010**, *55*, 1259−1265.
(18) Khan, M. S.; Husain, A. *Pharmazie* **2002**, *57*, 448−452.
(19) Leite, L.; Jansone, M.; Veveris, M.; Cirule, H.; Popelis, Y.; Melikyan, G.; Avetisyan, A.; Lukevics, E. *Eur. J. Med. Chem.* **1999**, *34*, 859−865.
(20) Klunk, W. E.; Covey, D. F.; Ferrendelli, J. A. *Mol. Pharmacol.* **1982**, *22*, 438−443.
(21) Ali, A. M.; Shahram, H.; Jamshid, C.; Ghadam Ali, K.; Farshid, H.; Fen-Tair, L.; Tai, W. L.; Kak-Shan, S.; Chi-Feng, Y.; Moti, L. J.; Ramasamy, K.; Cuihua, X.; Manijeh, P.; Gholam, H. *Bioorg. Med. Chem. Lett.* **2003**, *11*, 4303−4313.
(22) Wu, H.; Song, Z.; Hentzer, M.; Andersen, J. B.; Molin, S.; Givskov, M.; Høiby, N. *J. Antimicrob. Chemother.* **2004**, *53*, 1054−1061.
(23) Manefield, M.; Rasmussen, T.,B.; Henzter, M.; Andersen, J.,B.; Steinberg, P.; Kjelleberg, S.; Givskov, M. *Microbiology* **2002**, *148*, 1119−1127.
(24) Rasmussen, T. B.; Givskov, M. *Int. J. Med. Microbiol.* **2006**, *296* (2−3), 149−169.
(25) Kim, C.; Kim, J.; Park, H. -Y.; Park, H. -J.; Lee, J. H.; Kim, C. K.; Yoon, J. *Appl. Microbiol. Biotechnol.* **2008**, *80*, 37−47.
(26) Estephane, J.; Dauvergne, J.; Soulère, L.; Reverchon, S.; Queneau, Y.; Doutheau, A. *Bioorg. Med. Chem. Lett.* **2008**, *18*, 4321−4324.
(27) Defoirdt, T.; Miyamoto, C. M.; Wood, T. K.; Meighen, E. A.; Sorgeloos, P.; Verstraete, W.; Bossier, P. *Environ. Microbiol.* **2007**, *9*, 2486−2495.
(28) Defoirdt, T.; Crab, R.; Wood, T. K.; Sorgeloos, P.; Verstraete, W.; Bossier, P. *Appl. Environ. Microbiol.* **2006**, *72* (9), 6419−6423.
(29) Morohoshi, T.; Shiono, T.; Takidouchi, K.; Kato, M.; Kato, N.; Kato, J.; Ikeda, T. *Appl. Environ. Microbiol.* **2007**, *73*, 6339−6342.
(30) Manefield, M.; Harris, L.; Rice, S. A.; De Nys, R.; Kjelleberg, S. *Appl. Environ. Microbiol.* **2000**, *66*, 2079−2084.
(31) Abd-Alla, M. H.; Bashandy, S. R. *Int. Schol. Res. Net. (ISRN) Microbiol.* **2012**, *2012* (ArticleID 161890), 1−7.
(32) Ponnusamy, K.; Paul, D.; Kim, Y. S.; Kweon, J. H. *Braz. J. Microbiol.* **2010**, *41*, 227−234.
(33) Pèrez, A. G.; Olías, R.; Olías, J. M.; Sanz, C. *J. Agric. Food Chem.* **1999**, *47*, 655−658.
(34) Mahajan, V. A.; Borate, H. B.; Wakharkar, R. D. *Tetrahedron* **2006**, *62*, 1258−1272.
(35) Brouwer, H. D.; Schellekens, M. A.,J.; Klumperman, B.; Monteiro, M.,J.; German, A.,L. *J. Polym. Sci., Part A* **2000**, *38*, 3596−3603.
(36) Guha, S. K. U.S. Patent 5488075, 1996.
(37) Edgren, D.; Wong, P. S. L.; Theeuwes, F. U.S. Patent 4587117, 1986.
(38) Bellettini, A. G.; Bellettini, R. J. U.S. Patent 6210653, 2001.
(39) Zschoche, S.; David, R.; Tavana, H.; Pöschel, K.; Petong, N.; Dutschk, V.; Grundke, K.; Neumannb, A. W. *Colloids Surf. A* **2007**, *307*, 53−61.
(40) Saad, G. R.; Morsi, R. E.; Mohammady, S. Z.; Elsabee, M. Z. J. *Polym. Res.* **2008**, *15*, 115−123.
(41) Mpitso, K. Synthesis and characterization of styrene−maleic anhydride copolymer derivatives. M.Sc. Thesis, Stellenbosch University, Stellenbosch, South Africa, 2009.
(42) Varala, R.; Nuvula, S.; Adapa, S. R. *J. Org. Chem.* **2006**, *71*, 8283−8286.
(43) Claessens, S.; Naidoo, D.; Mulholland, D.; Verschaeve, L.; van Staden, J.; De Kimpe, N. *Synlett* **2006**, *4*, 621−623.
(44) Li, B.; Berliner, M.; Buzon, R.; Chiu, C. K.-F.; Colgan, S. T.; Kaneko, T.; Keene, N.; Kissel, W.; Le, T.; Leeman, K. R.; Marquez, B.; Morris, R.; Newell, L.; Wunderwald, S.; Witt, M.; Weaver, J.; Zhang, Z.; Zhang, Z. *J. Org. Chem.* **2006**, *71*, 9045−9050.
(45) Buttery, R. G.; Ling, L. C. *J. Agric. Food Chem.* **1996**, *44* (6), 1512−1514.
(46) Gule, N. P.; De Kwaadsteniet, M.; Cloete, T. E.; Klumperman, B. Fabrication and characterization of antibiofouling furanone modified nanofibers from poly(vinyl alcohol) via bubble electrospinning. In preparation.
(47) Aydilek, A. *J. Comput. Civil Eng. (ASCE)* **2002**, *16* (4), 280−290.
(48) Suwannakul, S.; Stafford, G. P.; Whawell, S. A.; Douglas, C. W. I. *Microbiology* **2010**, *156*, 3052−3064.
(49) Rojas-Chapana, J. A.; Correa-Duarte, M. A.; Ren, Z.; Kempa, K.; Giersig, M. *Nano Lett.* **2004**, *4* (5), 985−988.
(50) Zodrow, K.; Brunet, L.; Mahendra, S.; Li, D.; Zhang, A.; Li, Q.; Alvarez, P. J. J. *Water Res.* **2009**, *43*, 715−723.

(51) Close, D. M.; Xu., T.; Sayler., G. S.; Ripp., S. *Sensors* **2011**, *11*, 180−206.
(52) Cronin, M.; Akin, A. R.; Collins, S. A.; Meganck, J.; Kim, J.-B.; Baban, C. K.; Joyce, S. A.; van Dam, G. M.; Zhang, N.; van Sinderen, D.; O'Sullivan, G. C.; Kasahara, N.; Gahan, C. G.; Francis, K .P.; Tangney, M. *PLoS One* **2012**, *7* (1), 1−11.
(53) O'Neill, K.; Lyons, S. K.; Gallagher, W. M.; Curran, K. M.; Byrne, A. T. *J. Pathol.* **2010**, *220* (3), 317−327.
(54) Francis, D. L.; Visvikis, D.; Costa, D. C. *Eur. J. Nucl. Med. Mol. Imag.* **2003**, *30*, 988−994.
(55) Bshena, O. E. S. Synthesis of permanent non-leaching antimicrobial polymer nanofibers. Ph.D. Thesis, University of Stellenbosch, Stellenbosch, South Africa, 2012.
(56) Yun, K. M.; Suryamas, A. B.; Iskandara, F.; Bao, F. L.; Niinuma, H.; Okuyama, K. *Sep. Purif. Technol.* **2010**, *75*, 340−345.
(57) Lattmann, E.; Dunn, S.; Niamsanit, S.; Sattayasai, N. *Bioorg. Med. Chem. Lett.* **2005**, *15*, 919−921.
(58) Lonn-Stensrud, J.; Landin, M. A.; Benneche, T.; Petersen, F. C.; Scheie, A. A. *J. Antimicrob. Chemother.* **2009**, *63*, 309−316.
(59) Sindhu Ramachandran, C. V.; Sreekumar, P. K. *Int. J. Pharm. Pharm. Sci.* **2011**, *3*, 225−228.
(60) Weber, V.; Coudert, P.; Rubat, C.; Duroux, E.; Vallèe-Goyet, D.; Gardette, D.; Bria, M.; Albuisson, E.; Leal, F.; Gramain, J.-C.; Couqueleta, J.; Madesclaire, M. *Bioorg. Med. Chem.* **2002**, *10*, 1647−1658.
(61) Paulitz, T.; Nowak-Thompson, B.; Gamard, P.; Tsang, E.; Loper, J. *J. Chem. Ecol.* **2000**, *26* (6), 1515−1524.
(62) Hume, E. B. H.; Baveja, J. K.; Muirf, B.; Schubert, T. L.; Kumar, N.; Kjelleberg, S.; Griesser, H. J.; Thissen, H.; Read, R.; Poole-Warren, L. A.; Schindhelm, K.; Willcox, M. D. P. *Biomaterials* **2004**, *25*, 5023−5030.
(63) Sung, W. S.; Jung, H. J.; Park, K.; Kim, H. S.; Lee, I. S.; Lee, D. G. *Life Sci.* **2007**, *80*, 586−591.
(64) Kozminykh, V. O.; Igidov, N. M.; Kozminykh, E. N.; Semenova, Z. N.; Andreichikov, Y. S. *Pharmazie* **1992**, *47*, 261−263.
(65) Winzer, K.; Hardie, K. R.; Burgess, N.; Doherty, N.; Kirke, D.; Holden, M. T. G.; Linforth, R.; Cornell, K. A.; Taylor, A. J.; Hill, P. J.; Williams, P. *Microbiology* **2002**, *148*, 909−922.
(66) Kataoka, S. *J. Biosci. Bioeng.* **2005**, *100* (3), 227−234.